*Physiol Genomics* 57: 160–171, 2025.
*First published November 8, 2024; doi:10.1152/physiolgenomics.00072.2024*

american physiological society | PHYSIOLOGICAL GENOMICS

RESEARCH ARTICLE

# Ameliorating immune-dependent inflammation and apoptosis by targeting TLR4/MYD88/NF-κB pathway by celastrol mitigates the diabetic reproductive dysfunction

**Heba Faheem,[1] Rana Alawadhi,[2] Eman H. Basha,[1,3] Radwa Ismail,[4] Hoda A. Ibrahim,[5] Amira M. Elshamy,[5] Shaimaa M. Motawea,[4] Monira A. Seleem,[6] Alaa Elkordy,[7] Abdallah A. Homouda,[8] Howayda E. Khaled,[9] Reham A. Aboeida,[10] Muhammad T. Abdel Ghafar,[11] Fatma H. Rizk,[1] and Yasmeen M. El-Harty[1]**

[1]*Department of Physiology, Faculty of Medicine, Tanta University, Tanta, Egypt;* [2]*Science Department, College of Basic Education, PAAET, Ardhiya, Kuwait;* [3]*Department of Basic Medical Sciences–Physiology, Faculty of Medicine, Ibn Sina University for Medical Sciences, Amman, Jordan;* [4]*Department of Anatomy and Embryology, Faculty of Medicine, Tanta University, Tanta, Egypt;* [5]*Department of Medical Biochemistry, Faculty of Medicine, Tanta University, Tanta, Egypt;* [6]*Department of Medical Pharmacology, Faculty of Medicine, Tanta University, Tanta, Egypt;* [7]*Department of Neuropsychiatry, Faculty of Medicine, Tanta University, Tanta, Egypt;* [8]*Department of Urology, Faculty of Medicine, Tanta University, Tanta, Egypt;* [9]*Department of Zoology, Faculty of Science, Suez University, Suez, Egypt;* [10]*Department of Internal Medicine, Faculty of Medicine, Tanta University, Tanta, Egypt; and* [11]*Department of Clinical Pathology, Faculty of Medicine, Tanta University, Tanta, Egypt*

## Abstract

This study aimed to examine the protective effect of celastrol on testicular dysfunction in diabetic rats and the potential underlying mechanisms. All rats included in the study were divided into four groups: a control group treated with sodium citrate buffer and vehicle), a celastrol-treated control group, a streptozotocin (STZ)-induced diabetic group following insulin resistance, and a celastrol-treated diabetic group. Serum glucose, triglyceride, total cholesterol, high-density lipoprotein cholesterol, interleukin (IL)-1β, tumor necrosis factor-α, and testosterone levels were measured. In addition, the levels of testicular homogenate superoxide dismutase and malondialdehyde were assessed. Furthermore, testicular tissue relative toll-like receptor 4 (*TLR4*), nuclear factor kappa B (*NF-κB*), and myeloid differentiation factor 88 (*MYD88*) expressions were quantitatively measured using polymerase chain reaction. Histopathological and immunohistochemical studies were also conducted. The results revealed that treatment with celastrol significantly reduced *TLR4*, *MyD88*, and *NF-κB* expressions, and the levels of inflammatory mediators such as tumor necrosis factor-α and IL-1β in the testicular tissue of treated rats. These findings suggest that celastrol has the potential to be effective in the treatment of diabetes-induced testicular injury by inhibiting testicular inflammation, apoptosis, and oxidative stress.

**NEW & NOTEWORTHY** Celastrol inhibits the production of proinflammatory cytokines in the testicular tissue by specifically targeting the TLR4/MyD88/NF-κB signaling cascade pathways. This indicates that celastrol may serve as a promising new therapeutic target for treating diabetic reproductive dysfunction.

*celastrol; diabetic testicular dysfunction; TLR4/MYD88/NF-κB signaling pathway*

## INTRODUCTION

Diabetes mellitus (DM) is a prevalent and severe metabolic disease caused by impaired insulin function. It is associated with severe functional and structural issues, such as diabetic retinopathy, neuropathy, male impotence, and cardiovascular disease (1). DM has been found to induce fertility complications, including male reproductive organ dysfunction and infertility, due to its adverse effects on various organs, particularly the testis. It significantly reduces the diameter of seminiferous tubules, increases the number of testicular blood vessels, and alters the distribution of tubular stages (2).

Streptozotocin (STZ) is a glucosamine-nitrosourea compound derived from *Streptomyces achromogenes* that can induce DM. Pharmacologically, it is used as a chemotherapeutic agent for the treatment of pancreatic cell cancer, resulting in hypoinsulinemia and hyperglycemia. STZ exerts cytotoxic effects on pancreatic cells and harms various animal species, including rats, mice, and monkeys. However, it is most commonly used to induce DM in rats and mice (3).

Correspondence: Y. M. El-Harty (Yassmin.elharty@med.Tanta.edu.eg); E. H. Basha (Eman.basha@med.tanta.edu.eg).
Submitted 10 June 2024 / Revised 10 October 2024 / Accepted 10 October 2024

Diabetes can be caused by STZ in two different ways, depending on the dosage. It preferentially accumulates in cells by passing through the glucose transporter receptor, which is primarily expressed in β cells. STZ can bind to this receptor due to its structural similarity to glucose (4). STZ, which contains alkylating deadly nitrosourea molecules, selectively targets β cells when administered in a single high dose. Nevertheless, STZ induces an immunological and inflammatory response in diabetic rats and results in testicular dysfunction when administered in low, multiple doses. In addition, STZ has been associated with insulin resistance, which is widely known to induce adverse effects such as hepatotoxicity and nephrotoxicity (5).

To identify molecular patterns associated with pathogens produced by a variety of microorganisms, the innate immune system depends on the Toll-like receptor (TLR) family. In humans, the TLR family consists of 10 members (TLR1–10), whereas in mice, it comprises 12 members (TLR1–9 and TLR11–13) (6). Different TLRs attract adaptor molecules containing Toll-interleukin-1 receptor (TIR) domains, such as myeloid differentiation factor 88 (MyD88), TRIF, TIRAP/MAL, or TRAM. All TLRs use MyD88, which activates nuclear factor kappa B (NF-κB) and mitogen-activated protein kinases, inducing inflammatory cytokine gene expression. TIRAP functions as a sorting adapter that recruits MyD88 to cell surface Toll-like receptors (TLRs) like TLR2 and TLR4 (7).

In experimental models of diabetic liver injury, TLR4 has been identified as a receptor linked to whole body, low-grade chronic inflammatory diseases, and promotes macrophage infiltration. This mechanism is attributed to the transcription factor NF-κB, which is known for its involvement in the rapid synthesis of several cytokines associated with the immune and inflammatory systems (8). The TLR4 signaling pathway can activate NF-κB and induce the expression of proinflammatory genes (9).

Celastrol (C29H38O4) is a pentacyclic-triterpene extract derived from the roots of the traditional Chinese medicine plant *Tripterygium wilfordii* Hook F (TwHF, thunder god vine) (10). Recent advancements in research and signaling pathways have shown that celastrol effectively inhibits inflammation, insulin resistance, and other cardiometabolic problems by modulating various cellular responses (11, 12). In addition, it has been extensively utilized in the treatment of various disorders and diseases, including autoimmune diseases, cancer, and neurological diseases. Furthermore, celastrol has previously demonstrated efficacy in ameliorating cardiovascular disease caused by high fat intake and diabetic nephropathy (13). However, there is currently a scarcity of data regarding the protective effect of celastrol on testicular dysfunction associated with DM. Therefore, we conducted this study using a rat model to assess the protective effect of celastrol on testicular dysfunction associated with STZ-induced DM via different signaling pathways.

## MATERIALS AND METHODS

### Chemicals and Drugs

A purified celastrol solution was obtained from Sigma Chemical Co. (St. Louis, MO) and stored at −20°C. Before use, celastrol was dissolved in 10% dimethyl sulfoxide (DMSO), with a vehicle (distilled water containing 10% DMSO) serving as a control.

### Experimental Animals and Study Design

This study was conducted on 40 healthy male local strain Wister rats aged 4 wk and weighing ∼150–200 g, following the guidelines of our institution. The study was approved by the Research Ethics Committee of the Faculty of Medicine at Tanta University (Approval code number 35562/6/22). This study was conducted in accordance with the 1964 Declaration of Helsinki and its later amendments, as well as related ethical principles. All rats were obtained from a local vendor and placed in wire mesh cages on a 12-h light-dark cycle with free access to food and water for 1 wk before the experiment. Rats were then randomly divided into four equal groups (10 rats each) (Fig. 1):

1) Control group (*group I*): all rats in this group received a single intravenous injection of sodium citrate buffer and a vehicle of distilled water containing 10% DMSO for 8 wk.
2) Celastrol-treated group (*group II*): rats were raised in the same manner as the control group and received celastrol once daily at a dose of 500 μg/kg by oral gavage for 8 wk.
3) Diabetic group (*group III*): To establish a rat model of type 2 DM (T2DM), rats were fed a high-fat diet consisting of 10% sucrose, 10% lard, 1% cholesterol, and 0.3% sodium cholate. Following 8 wk of feeding, fasting serum glucose, and insulin levels (FINS, measured by radioimmunoassay), as well as triglyceride and total cholesterol levels, were assessed. The homeostatic model assessment for insulin resistance (HOMA-IR) and β-cell function (HOMA-B) were calculated as follows: (HOMA-IR = fasting serum glucose × FINS/22.5; HOMA-B = 20 × FINS/(fasting serum glucose − 3.5) (14). A single intravenous dose of STZ (15 mg/kg, pH 4.32) was administered upon the induction of insulin resistance (2, 15). Tail blood glucose was assessed, and levels >16.7 mmol/L indicated successful induction of the model.
4) Celastrol-treated diabetic group (*group IV*): rats were raised in the same manner as in the diabetic group. After confirmation of successful induction of T2DM in the eighth week, rats received celastrol once daily at a dose of 500 μg/kg by oral gavage for an additional 8 wk (16).

### Blood and Tissue Sampling

At the end of the experiment, after 8 wk for *groups I*, *II*, and *III* or after 16 wk for *group IV*, all animals were fasted overnight before anesthesia to collect blood samples by cardiac puncture. Blood was rapidly collected in a dry, well-sterile centrifugation tube and allowed to clot for 30 min at room temperature. Subsequently, the tube was centrifuged for 20 min (1,000 *g* at 4°C). Sera were collected and stored at −80°C for biochemical and immunochemical assays.

By the end of the experiment, all rats were euthanized after being anesthetized with an intraperitoneal dose of pentobarbital (50 mg/kg). Following a medial incision in the scrotum, the left and right testicles were exposed

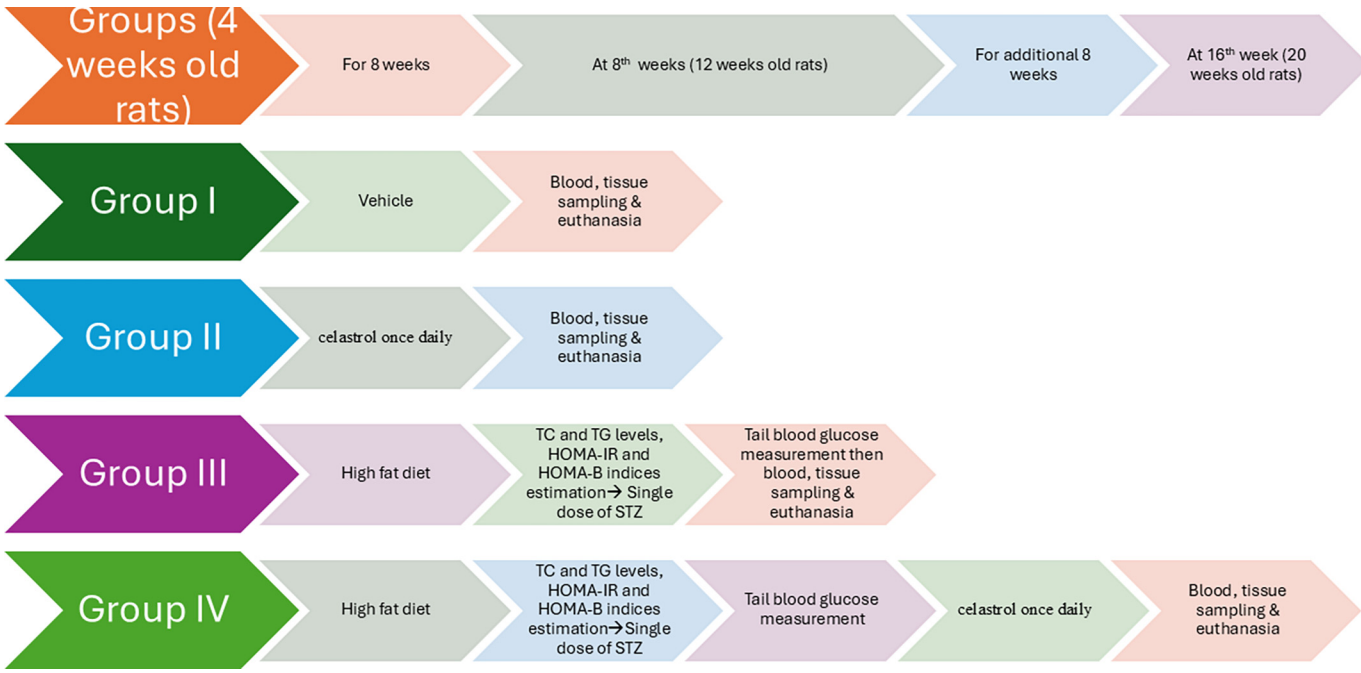


**Figure 1.** Summary of the timepoints of the study. HOMA-β, homeostatic model assessment for β-cell function; HOMA-IR, homeostatic model assessment for insulin resistance; STZ, streptozotocin; TC, total cholesterol; TG, triglyceride.

within the tunica vaginalis to prepare the testicular pairs. The testicles were quickly dissected, weighed, and then rinsed with saline (0.9% wt/vol) in their respective locations. Subsequently, they were left to dry by blotting with filter paper. The right testicles were frozen at −80°C for molecular analysis and tissue homogenate preparation. For histological and immunohistochemical analysis, the left testicles were fixed in a 10% neutral-buffered formalin solution (17).

The testicle tissue samples were defrosted, weighed, and then homogenized using a Potter–Elvehjem tissue homogenizer in 5 mL of cold phosphate-buffered saline (PBS; 50 mM; pH 7.4). The ratio of buffer to the tissue was 10:1 (mL/g). The suspension was then centrifuged at 5,000 *g* for 20 min at 4°C. Afterward, the supernatant was separated into aliquots and stored at −80°C for further analysis. Testicular tissue homogenates were assessed for total protein content using the technique by Lowry et al. (18).

### Biochemical Assays

The serum concentrations of glucose, total cholesterol (TC), triglyceride (TG), and high-density lipoprotein cholesterol (HDL-C), as well as testicular homogenate superoxide dismutase (SOD) and malondialdehyde (MDA), were determined using commercially available kits (Cat. Nos. GL 13 20, CH 12 20, TR 20 30, CH 12 30, SD 25 21, and MD 25 29, respectively; Bio-diagnostic, Giza, Egypt). The concentrations of low-density lipoprotein cholesterol (LDL-C) were calculated as follows: LDL-C = TC − (TG/5) − HDL (19).

**Table 1.** *Primer sequences for real-time polymerase chain reaction*

| Gene | Primer Sequence |
|---|---|
| TLR4 | Forward 5′-ATGAGGACTGGGTGAGAAAC-3′<br>Reverse 5′-CACCACCACAATAACTTTCC-3′ |
| NFKB | Forward 5′-AAAAACGCATCCCAAGGTGC-3′<br>Reverse 5′-AAGCTCAAGCCACCATACCC-3′ |
| MYD88 | Forward 5′-TGGTGGTTGTTTCTGACGAT-3′<br>Reverse 5′-CGCAGATAGTGATGAACCGT-3′ |
| GAPDH | Forward 5′-GCAAGTTCAACGGCACAG-3′<br>Reverse 5′-GCCAGTAGACTCCACGACAT-3′ |

### Enzyme-Linked Immunosorbent Assay

The serum levels of interleukin 1β (IL-1β), tumor necrosis factor-α (TNF-α), reactive oxygen species (ROS), and testosterone were measured using commercially available ELISA kits (Cat. Nos. MBS702717, MBS282960, MBS039665, and MBS282195, respectively; MyBioSource, Inc., Southern California, San Diego, CA), following the manufacturer's instructions. The microplates were read using a microplate reader (Stat Fax 2100, Fisher Bioblock Scientific, France) at a wavelength of 450 nm with a correction at 570 nm.

The intra-assay precision coefficient variation (CV%) for interleukin 1β (IL-1β), tumor necrosis factor-α (TNF-α), and testosterone was <8, <8, and <15%, respectively. Inter-assay precision coefficient variation (CV%) for interleukin 1β (IL-1β), tumor necrosis factor-α (TNF-α), and testosterone was <10, <12, and <15%, respectively.

The serum levels of toll-like receptor 4 (TLR4), nuclear factor kappa B (NF-κB), and myeloid differentiation factor 88 (MYD88) were measured using commercially available ELISA kits (Cat. Nos. MBS452190, MBS287521, and MBS455709, MyBioSource, Inc., Southern California, San Diego, CA), following the manufacturer's instructions.

The intra-assay precision coefficient variation (CV%) for TLR4, NF-κB, and MYD88 was <10, <8, and <10%, respectively. The intra-assay precision coefficient variation (CV%)

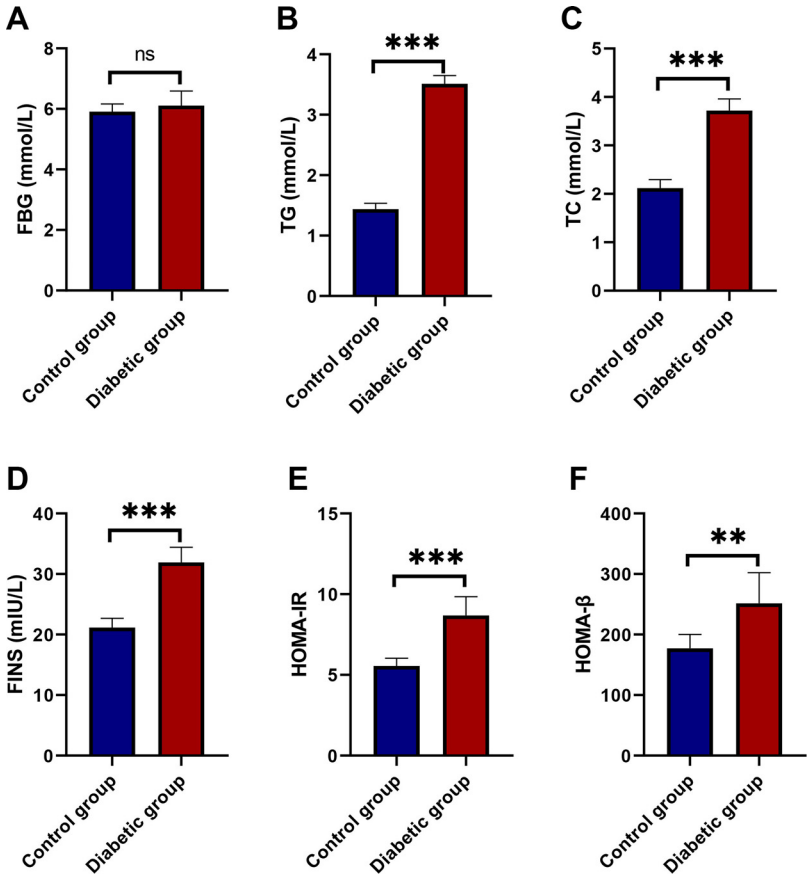


**Figure 2.** Indices of glucose and β-cell function following a high-fat diet for 8 wk. There are 10 rats in each of the control and diabetic groups. The data are presented as means ± SD of (*A*) fasting blood glucose (FBG), (*B*) triglyceride (TG), (*C*) total cholesterol (TC), (*D*) fasting insulin (FINS), and insulin resistance. (*F*) HOMA-β, homeostatic model assessment for β-cell function; (*E*) HOMA-IR, homeostatic model assessment for insulin resistance; ***Significant change ($P < 001$).; ns, not significant.

for TLR4, NF-κB, and MYD88 was <12, <12, and <12%, respectively.

### Quantitative Real-Time Reverse Transcription PCR Assays

Total RNA was isolated after frozen testicular homogenate using the RNeasy Total RNA isolation Kit (Qiagen, Hiden, Germany) according to the manufacturer's instructions. cDNA was then synthesized using the SuperScript III First-Strand Synthesis System for the quantitative real-time reverse transcription PCR (rt-PCR) kit (Life Technologies Co., Carlsbad, CA) following the manufacturer's instructions. The PCR was performed using the PCR Master Mix Power SYBR Green (Life Technologies Co., Carlsbad, CA), following the manufacturer's guidelines. Internal control was established using the housekeeping gene GAPDH to normalize the mRNA transcripts of *TLR4*, *NF-κB*, and *MYD88*. Sequence-specific primers were designed as displayed in Table 1. The

**Table 2.** *Rat physical and biochemical parameters examined in this research*

| | *Group I* (*n* = 10) | *Group II* (*n* = 10) | *Group III* (*n* = 10) | *Group IV* (*n* = 10) |
|---|---|---|---|---|
| Body weight, g | 453.9 ± 7.62$^{c,d}$ | 452.7 ± 7.02$^{c,d}$ | 285.2 ± 7.05$^{a,b,d}$ | 339 ± 8.72$^{a,b,c}$ |
| Glucose, mmol/L | 6.04 ± 0.13$^{c,d}$ | 5.95 ± 0.2$^{c,d}$ | 28.25 ± 1.5$^{a,b,d}$ | 22.5 ± 1.18$^{a,b,c}$ |
| TG, mmol/L | 1.62 ± 0.15$^{c,d}$ | 1.55 ± 0.14$^{c,d}$ | 4.25 ± 0.14$^{a,b,d}$ | 3.13 ± 0.19$^{a,b,c}$ |
| TC, mmol/L | 2.23 ± 0.13$^{c,d}$ | 2.1 ± 0.11$^{c,d}$ | 6.44 ± 0.25$^{a,b,d}$ | 5.32 ± 0.17$^{a,b,c}$ |
| HDL-C, mmol/L | 0.58 ± 0.06 | 0.55 ± 0.18 | 0.49 ± 0.074 | 0.53 ± 0.067 |
| LDL-C, mmol/L | 1.33 ± 0.16$^{c,d}$ | 1.24 ± 0.16$^{c,d}$ | 5.1 ± 0.26$^{a,b,d}$ | 4.16 ± 0.17$^{a,b,c}$ |
| SOD, U/mg protein | 7.38 ± 0.15$^{c,d}$ | 7.44 ± 0.12$^{c,d}$ | 3.27 ± 0.13$^{a,b,d}$ | 6.49 ± 0.07$^{a,b,c}$ |
| MDA, mmol/g tissue | 8.15 ± 0.17$^{c,d}$ | 8.14 ± 0.18$^{c,d}$ | 14.03 ± 0.22$^{a,b,d}$ | 10.06 ± 0.18$^{a,b,c}$ |
| ROS, U/mL | 62.5 ± 4.93$^{c,d}$ | 63.6 ± 6.35$^{c,d}$ | 355 ± 20.75$^{a,b,d}$ | 233.7 ± 9.81$^{a,b,c}$ |
| Testosterone, ng/mL | 7.49 ± 0.38$^{c,d}$ | 7.5 ± 0.32$^{c,d}$ | 3.7 ± 0.23$^{a,b,d}$ | 6.74 ± 0.88$^{a,b,c}$ |
| TNF-α, ng/mL | 52.69 ± 0.38$^{c,d}$ | 52.61 ± 0.46$^{c,d}$ | 86.18 ± 3.01$^{a,b,d}$ | 64.94 ± 14.11$^{a,b,c}$ |
| IL-1β, ng/mL | 23.74 ± 0.69$^{c,d}$ | 23.67 ± 0.2$^{c,d}$ | 53.3 ± 0.79$^{a,b,d}$ | 34.29 ± 0.87$^{a,b,c}$ |

There are 10 rats in each group. The data are presented as means ± SD and were compared using a one-way analysis of variance with Tukey's post hoc test. *$P < 0.05$ indicates a significant difference between the groups. HDL-C, high-density lipoprotein cholesterol; IL-1β, interleukin-1β; LDL-C, low-density lipoprotein cholesterol; MDA, malondialdehyde; ROS, reactive oxygen species; SOD, superoxide dismutase; TC, total cholesterol; TG, triglyceride; TNF-α, tumor necrosis factor-alpha. The degree of freedom is 3 between groups and 36 within groups (total = 39). [a]Significance from *group I*. [b]Significance from *group II*. [c]Significance from *group III*. [d]Significance from *group IV*.

relative gene expression was determined by the $2^{-\Delta\Delta CT}$ formula (20).

### Histopathological and Immunohistochemical Assays

Left testicles were processed into paraffin blocks and cut into 5-μm-thick tissue sections. The sections were stained with hematoxylin and eosin (H&E) stain (21). Before immunohistochemical staining, testicular sections that were embedded in 5-mm-thick paraffin were dewaxed and then rehydrated in a descending series of alcohols. The sections were incubated in 3% hydrogen peroxide for 30 min to inhibit endogenous peroxidase activity. Antigen retrieval was performed in a microwave oven for 10 min. To reduce nonspecific binding, the sections were rinsed with PBS. The sections were blocked with 5% bovine serum at room temperature. They were subsequently treated with specific primary antibodies: anti-caspase-3 (1:100; Cat. No. ab2302; Abcam, Cambridge, UK), mouse monoclonal anti-CD68 antibody (1:100 in PBS; Cat. No. ab283654; Abcam, UK) and anti-cleaved caspase-3 antibody (1:20; Cat. No. AB3623, Merck Millipore, Billerica, MA). The sections were then counterstained with hematoxylin after being rinsed twice. The immunohistochemical reactivity was revealed at a concentration of 0.06% of 3.3′-diaminobenzidine (DAB) (Dako). The sections were then dehydrated in a series of xylene and ethanol for 2 min at 70, 90, and 100%. The sections were subsequently examined using an Olympus BX 50 Automated light microscope, and photographs were captured with an Olympus digital video camera (22, 23).

### Morphometric Study

Ten nonoverlapping random fields were selected from testicular slices and submitted for morphometric analysis using ImageJ software from Media Cybernetics (magnification: ×400). The thickness of seminiferous tubular germinal epithelium, the ratio of germinal epithelium (GE) thickness to seminiferous tubules (ST) diameter, optical color density of anti-caspase-3 immunoexpression, and the mean area percentage of anti-CD68 immunoexpression were measured.

### Statistical Analysis

The results were presented as means ± SD and compared using a one-way analysis of variance (ANOVA) with Tukey's

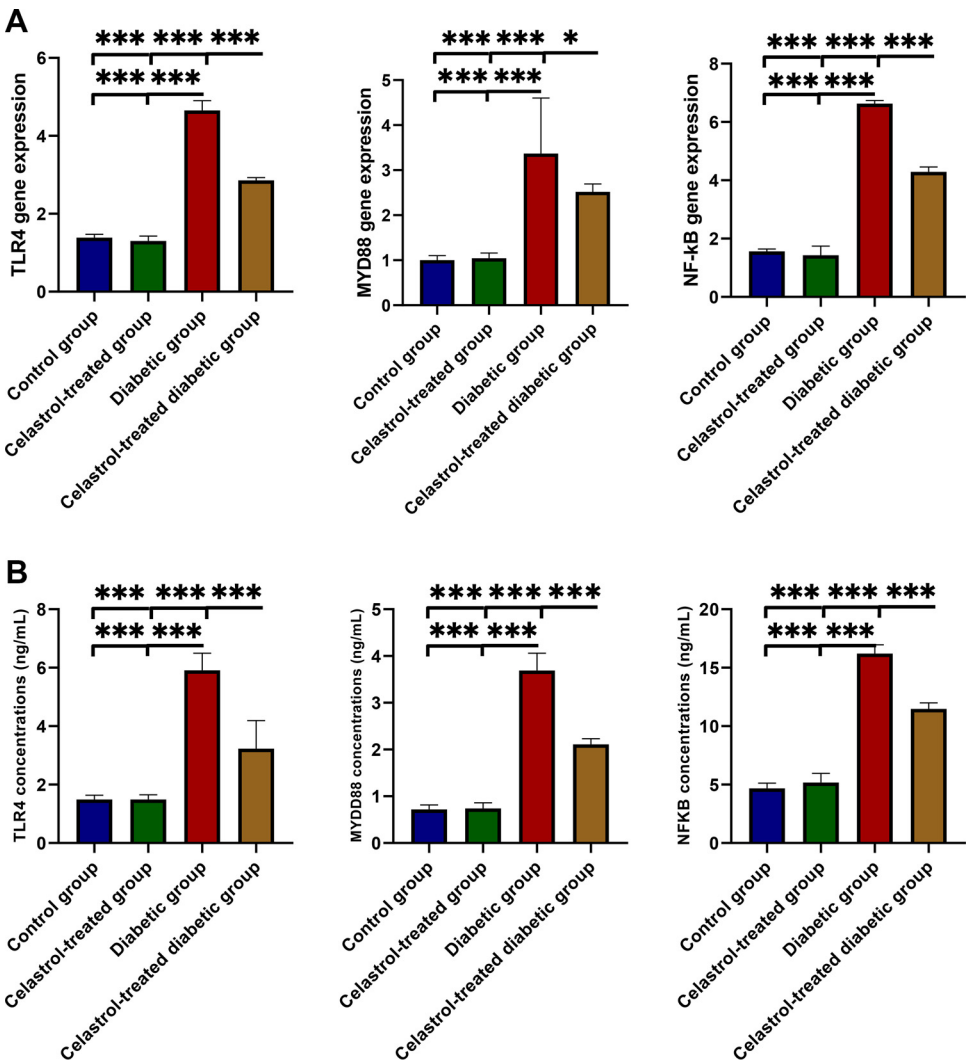


**Figure 3.** Comparison among the studied groups in terms of: the relative gene expression of toll-like receptor 4 (*TLR4*), myeloid differentiation factor 88 (*MYD88*), and nuclear factor kappa B (*NF-κB*; *A*), comparison among the studied groups shows the change in the protein level of *TLR4*, *MYD88*, and *NF-κB* (*B*). There are 10 rats in each group. The data are presented as means ± SD and were compared using a one-way analysis of variance with Tukey's post hoc test. Significance of change: $^{*}P < 0.05$, $^{***}P < 0.001$.

post hoc test. The level of statistical analysis was set at a $P$ value of $<0.05$. Data analysis was performed using the Statistical Package for the Social Sciences (SPSS) software Version 23.0 (IMB, New York), and graphs were generated using GraphPad Prism software Version 9.3.1 (Boston, MA).

## RESULTS

### Parameters following an 8 wk of High-Fat Diet

The TC and TG levels, as well as the HOMA-IR and HOMA-B indices, were significantly higher in rats fed on a high-fat diet than in the normal control group. However, there were no changes in serum glucose levels. These findings indicate that insulin resistance was induced after 8 wk of following a high-fat diet (Fig. 2).

### Potential Impact of Celastrol on Physical and Biochemical Parameters Measured at the End of the Experiment

Table 2 summarizes the physical and biochemical characteristics of different rat groups. With regard to all parameters examined in this experiment, there were no statistically significant differences between the normal control and celastrol-treated control groups.

In comparison with the normal control group, diabetic rats exhibited significantly decreased body weights. In addition, their levels of serum glucose, TG, TC, LDL-C, MDA, TNF-α, and IL-1β were significantly higher compared with the other studied groups. However, the levels of SOD and testosterone were significantly lower in the diabetic rat group compared with the other studied groups ($P < 0.001$). There were no significant differences in HDL-C levels among all studied groups ($P < 0.05$).

Celastrol-treated diabetic rats demonstrated a significant reduction in serum glucose levels compared with the diabetic rat group. In addition, celastrol-treated diabetic rats showed improvements in SOD levels and lipid profile, as well as MDA, TNF-α, and IL-1β levels, compared with the diabetic rat group ($P < 0.001$).

### The Potential Impact of Celastrol on mRNA Gene Expression of *TLR4*, *MYD88*, and NF-κB and Their Protein Level Measured at the End of the Experiment

There was no significant difference in the relative testicular mRNA expression and protein level of *TLR4*, *MYD88*, and *NF-κB* between the normal control and celastrol-treated control groups. There was a statistically significant increase in the relative testicular mRNA expression and protein level of *TLR4*, *MYD88*, and *NF-κB* in the diabetic rat group compared with the other studied groups ($P < 0.001$). Nevertheless, the celastrol-treated diabetic rats showed a significant decrease in the relative testicular mRNA expression and protein level of *TLR4*, *MYD88*, and *NF-κB* compared with the diabetic rat group (Fig. 3).

### The Potential Impact of Celastrol on Histological, Immunohistochemical, and Morphometric Findings Measured at the End of the Experiment

The H&E sections revealed that the seminiferous tubules in both the normal control and celastrol-treated control group displayed a normal structure with mature sperms and layers of germ cells with full thickness. The interstitial tissue also had a normal structure with normal interstitial cells and associated blood vessels. In the diabetic group, there was hyperplasia of Leydig cells in the interstitial tissue and congested blood vessels. Furthermore, the seminiferous tubules experienced substantial degeneration and loss of germ cell layers, resulting in the detachment of the germinal epithelium from their basement membranes. However, in the celastrol-treated diabetic group, the testicular parenchyma and interstitial tissue showed restoration of normal structure with a few tubules with degenerated cells and mild interstitial edema (Fig. 4).

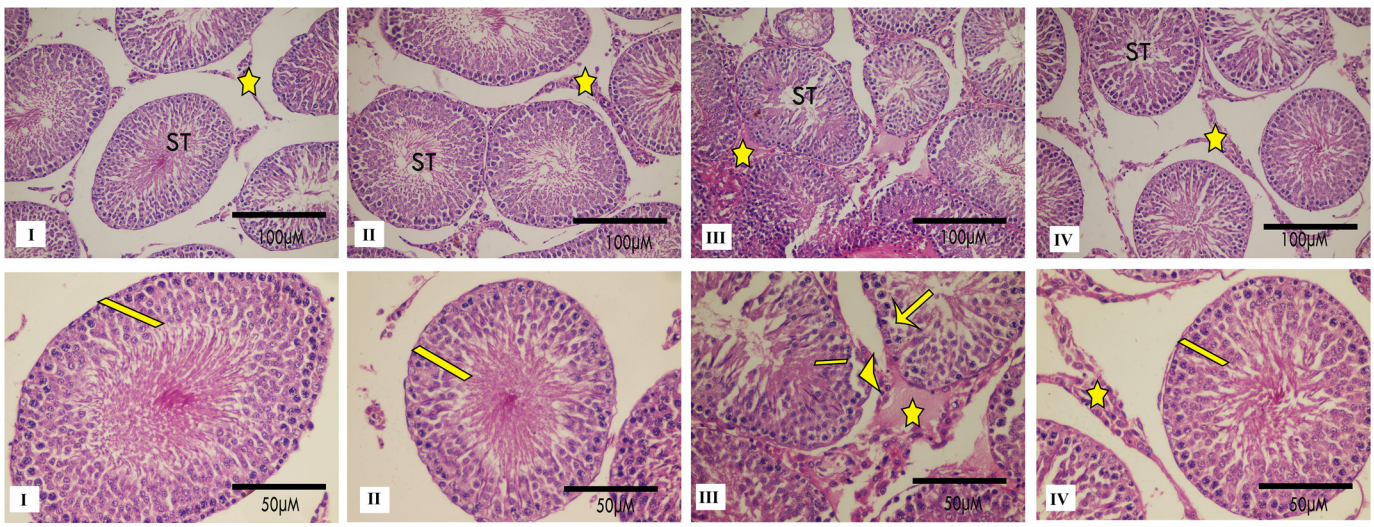


**Figure 4.** Hematoxylin and eosin (H&E) sections of the rat testis. The normal control and celastrol-treated control *groups I* and *II*, show normal seminiferous tubules with mature sperms [seminiferous tubules (ST)] and germ cell layers with full-thickness (thick line) and normal structure of interstitial tissue (star). The diabetic *group III* shows loss of germ cell layers with degeneration (arrow), detached germinal epithelium from their basement membranes (head arrow), and hyperplasia of Leydig cells in the interstitial tissue with congested blood vessels (star). The normal structure of the ST with few degenerated cells and mild interstitial edema (star) is seen in celastrol-treated diabetic *group IV* (first row: H&E ×200; scale bar: 100 μm; second row: H&E ×400; scale bar: 50 μm).

The thickness of the germinal epithelium in the seminiferous tubules and the ratio of GE thickness to ST diameter were significantly decreased in the diabetic group (30.96 ± 2.58; 9.55 ± 0.73, respectively) than in the normal control group (70.82 ± 5.06; 25.37 ± 0.98, respectively; $P < 0.05$). However, they were significantly increased in the celastrol-treated diabetic group (49.48 ± 1.69; 20.68 ± 0.68, respectively) than in the diabetic group (30.96 ± 2.58; 9.55 ± 0.73, respectively; $P < 0.05$; Fig. 5).

The normal control and celastrol-treated control group exhibited a faint cytoplasmic reaction in the caspase-3 immunostained sections. In the diabetic group, there was an increase in caspase-3 expression. Nevertheless, in the celastrol-treated diabetic group, there was a mild-to-moderate cytoplasmic reaction observed (Fig. 6). Furthermore, the caspase-3 optical density was found to be significantly increased in the diabetic group (0.775 ± 0.047) compared with the normal control group (0.509 ± 0.03; $P < 0.05$). However, the caspase-3 optical density markedly decreased in the celastrol-treated diabetic group (0.625 ± 0.042) compared with the diabetic group (0.775 ± 0.047; $P < 0.05$; Fig. 5).

The immunohistochemical analysis of CD68 in the normal control and celastrol-treated control group showed a positive reaction in the cytoplasm of macrophages present in the interstitium between seminiferous tubules. In the diabetic group, there was a strong positive reaction in CD68 immunoreactivity sections. However, in the celastrol-treated diabetic group, there was minimal positive cytoplasmic reactivity observed (Fig. 7). The mean area percentage of CD68 immunoreaction was significantly higher in the diabetic group (59.04 ± 1.76) than in the normal control group (20.05 ± 0.797; $P < 0.05$). The CD68 mean area percentage in the celastrol-treated diabetic group (41.35 ± 1.69) significantly decreased compared with the diabetic group (59.04 ± 1.76; $P < 0.05$; Fig. 5).

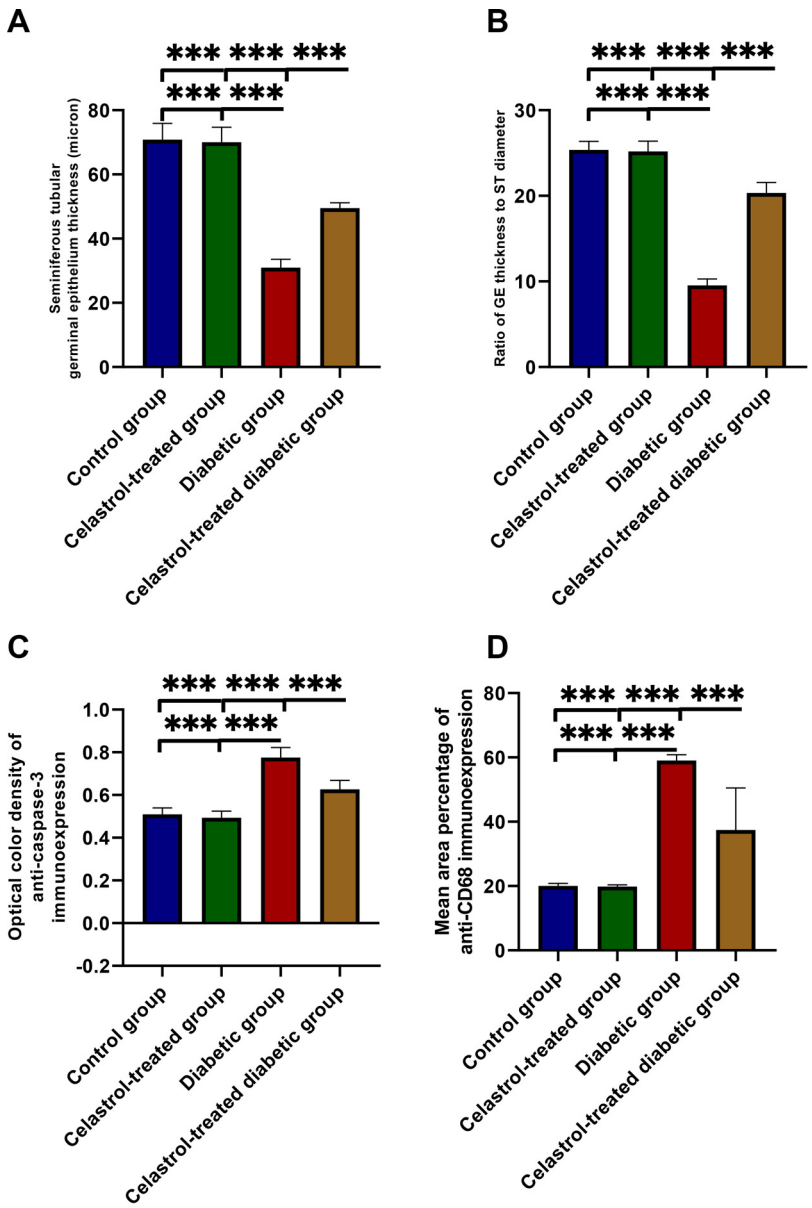


**Figure 5.** Morphometric parameters for rats evaluated in this study, including the thickness of the seminiferous tubular germinal epithelium (*A*), the ratio of germinal epithelium (GE) thickness to seminiferous tubules (ST) diameter (*B*), the optical color density of the anti-caspase-3 immunoexpression (*C*), and the mean area percentage of the anti-CD68 immunoexpression (*D*). There are 10 rats in each group. The data are presented as means ± SD and were compared using a one-way analysis of variance with Tukey's post hoc test. ***Significance of the change ($P < 0.001$).

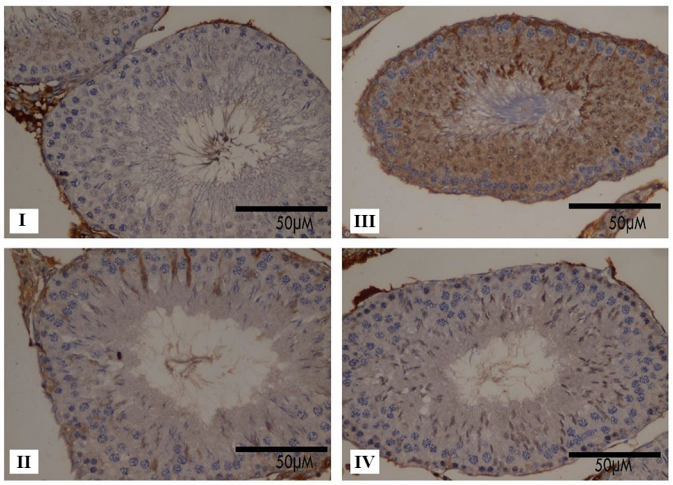


**Figure 6.** Immunohistochemical analysis of caspase-3 expression. In the normal control and celastrol-treated control *groups I* and *II*, caspase-3 immunostained sections reveal a faint cytoplasmic reaction. The diabetic *group III* shows an increase in caspase-3 immunoreactivity sections. The celastrol-treated diabetic *group IV* shows a mild cytoplasmic reaction (caspase-3 ×400; scale bar: 50 μm).

The germ cells in both the normal control and celastrol-treated control groups exhibited faint staining of cleaved caspase-3. The diabetic group showed strong immunoreactivity of cleaved caspase-3. The celastrol-treated diabetic group showed a mild immunoreactivity of cleaved caspase-3 (Fig. 8).

## DISCUSSION

Diabetes can have detrimental effects on numerous organs and tissues, leading to a variety of complications in the skin, blood vessels, neurological system, liver, and kidneys (24). Specifically, chronic hyperglycemia disrupts the normal functioning of the reproductive system and affects sexual behavior and male reproductive processes, resulting in decreased fertility. Diabetic testicular damage can be either temporary or permanent, depending on the severity and duration of the condition (25).

In the present study, we observed the development of insulin resistance following an 8-wk period of high-fat feeding, as evidenced by an increase in serum insulin, TC, and TG levels, as well as HOMA-IR and HOMA-B indices in the high-fat diet group compared with normal the control group. However, there were no changes in serum glucose levels between the two groups. This finding can be elucidated by the presence of hyperinsulinemia, which is similar to the prediabetic state in humans. This process helps maintain normal glucose homeostasis as a compensatory mechanism for impaired insulin sensitivity (11).

Numerous investigations have revealed that oxidative stress, inflammation, and apoptosis are the primary triggers of male diabetic testicular injury (26). Natural anti-inflammatory solutions are reliable alternatives to traditional approaches to controlling inflammatory illnesses. Celastrol is a plant-based anti-inflammatory substance that has been used in traditional medicine for centuries. Although celastrol has been examined, its potential to reduce inflammation and ameliorate testicular damage induced by diabetes remains unclear. In this study, we investigated the effect of celastrol on the inflammatory response in a diabetic rat model. Previous studies have reported that diabetes decreases body weight in rats (16, 27, 28). Similarly, our results showed that body weight was lower in the diabetic group than in the normal control and celastrol-treated control groups. As previously reported (28), celastrol treatment significantly improved body weight in the celastrol-treated diabetic group compared with the untreated diabetic group.

Our results indicated that diabetic rats exhibited altered lipid profiles, elevated glucose levels, and insulin resistance compared with the normal control and celastrol-treated control groups. However, celastrol treatment improved all of these parameters in the celastrol-treated diabetic group

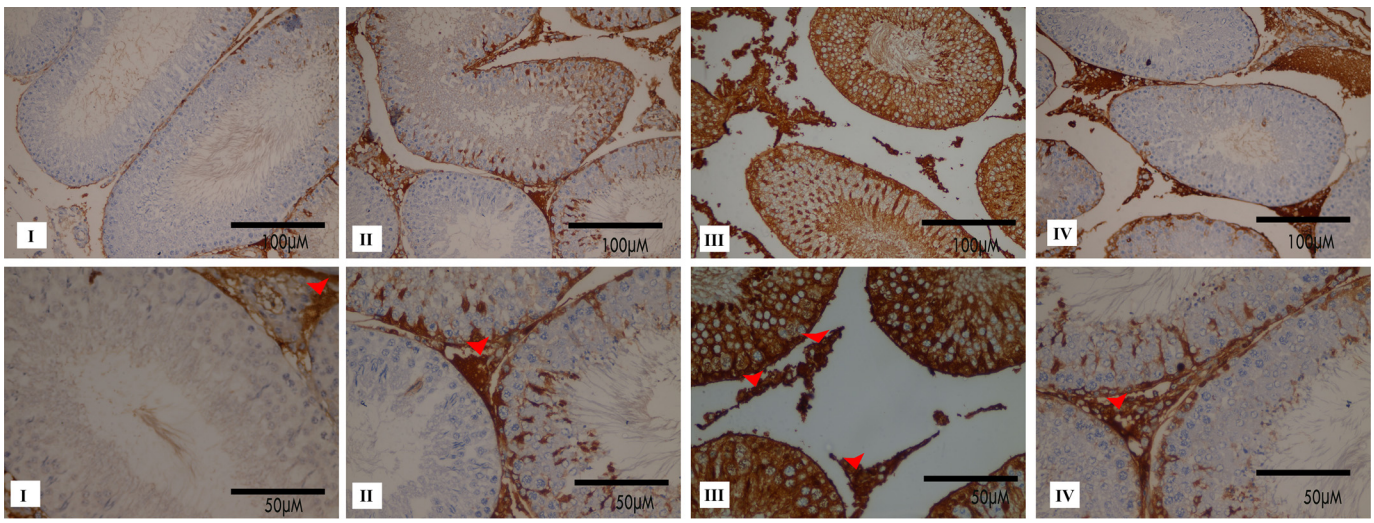


**Figure 7.** Immunohistochemical analysis of CD68 expression. In the normal control and celastrol-treated control *groups I* and *II*, CD68 immunostained sections reveal a positive reaction in the cytoplasm of macrophages present in the interstitium in between seminiferous tubules (head arrow). The diabetic *group III* shows a strong positive reaction in CD68 immunoreactivity sections. The celastrol-treated diabetic *group IV* shows a mild positive cytoplasmic reaction (first row: CD68 ×200; scale bar: 100 μm; second row: CD68 ×400; scale bar: 50 μm).

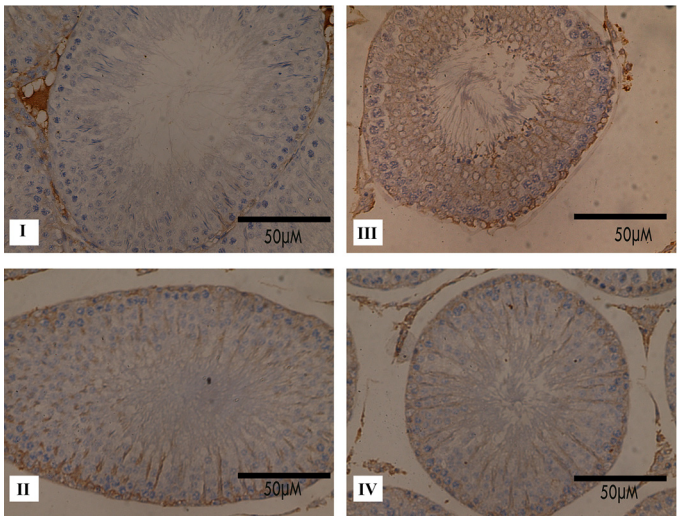


**Figure 8.** Immunohistochemical analysis of cleaved caspase-3 expression. In the normal control and celastrol-treated control *groups I and II*, immunostained sections reveal faint staining. The diabetic *group III* shows strong immunoreactivity of cleaved caspase-3. The celastrol-treated diabetic *group IV* shows a mild immunoreactivity of cleaved caspase-3 (cleaved caspase-3 ×400; scale bar: 50 μm).

compared with the untreated diabetic group. This beneficial effect has been observed in cases of inflammation and insulin resistance caused by a high-fructose diet in rat adipose tissue (29).

Hyperglycemia-induced oxidative stress can be attributed to various hypothetical factors, such as glucose auto-oxidation, nonenzymatic glycation, the interaction between glycated products and their receptors, excessive generation of reactive oxygen species (ROS) by mitochondria, and the activation of the polyol pathway (30). Furthermore, hyperglycemia has been found to activate specific metabolic pathways, including NADPH-oxidase, protein kinase C, and diacylglycerol, resulting in ROS generation. This pathway has previously been referred to as the "risky metabolic pathway in diabetes" (31).

Male infertility is significantly influenced by hyperglycemia, which is linked to reproductive issues, particularly testicular failure. Leydig cells, the main cell type in the testis interstitium, play a crucial role in the regulation of testis homeostasis and can trigger an immune response upon stimulation. It is well established that hyperglycemia can modulate the activity of the innate immune receptor TLR4 in different cell populations and tissues. The activation of TLR4 in testicular cells, particularly Leydig cells, by hyperglycemia can lead to the development of oxidative stress and inflammation, both of which contribute to testicular dysfunction (32).

Sertoli cells, which express various TLRs, including TLR4, the lipopolysaccharide receptor, are also involved in testicular inflammation. Activation of these TLRs by legends triggers inflammatory signaling pathways in Sertoli cells. This results in the activation of NF-κB and mitogen-activated protein kinases, which are inflammatory transcription factors (33).

The TLR4 pathway is a potential candidate for triggering a proinflammatory response. It can be activated by lipopolysaccharides and harmful metabolic products, leading to the activation of downstream molecules such as MyD88. This promotes the nuclear translocation of the transcription factor NF-κB and the production of cytokines and chemokines associated with inflammation, including IL-1 and TNF-α (34). In addition, proinflammatory chemokines can enhance NF-κB activation, acting as a positive feedback regulator and amplifying the inflammatory response (35).

Inflammation can induce cell damage, which in turn exacerbates oxidative stress. Oxidative stress can also stimulate inflammation. Phagocytic cells activate NOX, which releases ROS, to eliminate pathogens during an inflammatory response. In addition, ROS can attract certain immune cells, such as neutrophils and monocytes, thereby impacting the progression of inflammatory responses (36, 37).

The generation of damage-associated molecular pattern molecules (DAMPs) under oxidative stress has been demonstrated to activate the TLR family of receptors. The release of DAMPs during ischemia insults can promote inflammation, potentially through TLR activation. In contrast, TLR4 activation can also lead to the release of DAMPs, creating a paracrine loop that amplifies inflammation and causes damage to the affected organ. Evidence indicates that activation of TLR4 can trigger ROS signaling by directly interacting with NADPH oxidase (38).

Studies on the acute kidney injury model have demonstrated that oxidative stress can lead to apoptosis. For instance, in the presence of oxidative stress, direct mitochondrial activation by ROS can increase the Bax/Bcl-2 ratio, which in turn increases the permeability of the mitochondrial membrane. This can trigger apoptosis through caspase-dependent or independent mechanisms (39).

Inhibition of the TLR4 signaling pathway has been shown to significantly reduce the expression of cleaved caspase-3, Bcl-2, Bax, and other apoptosis-related proteins in the rat brain (40). Therefore, targeting the TLR4 pathway may offer a potential intervention strategy for managing diabetic testicular dysfunction.

Our findings revealed that the expression of *TLR4*, *MyD88*, and *NF-κBp65* genes was consistently increased in the testes of diabetic rats. However, the administration of celastrol led to a reduction in the expression of these genes, suggesting the possible anti-inflammatory activity of celastrol. This effect may be attributed to a signal transduction pathway that relies on the *TLR4*/*MyD88* genes. Consistent with this hypothesis, the levels of proinflammatory cytokines IL-1β and TNF-α were significantly increased in the untreated diabetic group compared with the normal control and celastrol-treated control groups. However, treatment with celastrol in diabetic rats reduced the levels of these cytokines. The previous literature has documented the anti-inflammatory effect of celastrol (41–44).

In DM, increased lipid peroxidation causes an increase in MDA synthesis in the testicles, while depletion of antioxidants, such as SOD activity, leads to oxidative damage (45). Consistent with these findings, our study revealed that SOD levels were lower in the untreated diabetic group than in the normal control and celastrol-treated control group, whereas MDA levels were higher. However, treatment with celastrol in diabetic rats increased SOD levels and decreased MDA levels. The previous literature has documented the antioxidant activity of celastrol (42, 46, 47).

Significant reductions in testicular and plasma testosterone levels were observed in STZ-induced diabetic rats as compared with the normal controls (48). The reduction of testosterone in testis might play a role in diabetic impotence (49). The present study revealed a comparable effect of diabetes on serum testosterone levels, whereby the untreated diabetic group exhibited a decline in comparison with both the normal control and celastrol-treated control groups. Administration of celastrol resulted in an increase in serum testosterone levels in the celastrol-treated diabetic group compared with the untreated one.

In our study, celastrol demonstrated a substantial ability to decrease the immune response to testicular inflammation. As the deterioration of diabetic testicular function advanced, the TLR4/MyD88/NF-κB pathway triggered the inflammatory pathways, leading to the chemotactic motion and aggregation of macrophages and other killer cells.

In this study, histological analysis of the testis (seminiferous tubules) in rats revealed significant degenerative changes associated with diabetes. These changes involved the detachment of germinal epithelium from their basement membranes and hyperplasia of Leydig cells in the interstitial tissue. Comparable findings have been reported by Al-Khamas (50), who described vacuolation in the seminiferous tubules and degeneration of interstitial Leydig cells in rats induced with alloxan-induced diabetes. In addition, Faddladdeen (51) observed significant vacuolar and degenerative alterations in the seminiferous tubules of rats-induced STZ-induced diabetes. Furthermore, there was a marked decrease in the mean thickness of the germ cell layers compared with controls. The administration of celastrol preserved and restored the natural seminiferous tubule structure in diabetic rats, protecting the full thickness of the germ cell layers.

Caspase-3 immunostaining was utilized to demonstrate apoptosis in spermatogenic cells, as shown on H&E-stained slides. Upregulation of caspase-3 expression was observed in the seminiferous tubules of diabetic rats. However, in groups receiving celastrol, caspase-3 expression was almost completely restored to normal levels. According to Harakeh et al. (52), diabetic sections (high-fat diet + STZ) exhibited higher levels of caspase-3 immunoexpression in the damaged tubular nuclei compared with the control section. These findings demonstrate a correlation between diabetes caused by a high-fat diet + STZ and caspase-3-mediated apoptosis in the rat's testis. In a study examining the neuroprotective effects of celastrol in parkinsonism, Zhang et al. (53) found that celastrol-induced Nrf2 and decreased NLRP3 and caspase-1. This finding is relevant to the observed improvement in caspase-3 expression in the celastrol-treated group in the current study. In this study, CD68 immunostaining was used as a macrophage marker. The CD68 immunoreactivity sections of the untreated diabetic group exhibited a strong positive reaction. However, the celastrol-treated groups restored this expression to nearly normal levels. Triptolide and celastrol are effective diabetes medications that can lower blood sugar, enhance mitochondrial activity, improve kidney function, reduce inflammation, and delay renal damage (54). Recent studies have demonstrated that celastrol significantly reduces synovial hyperplasia, inflammatory cell infiltration, joint edema, arthritis index scores, and serum IL-1 and IL-18 secretion in rats exposed to complete Freund's adjuvant (55).

### Conclusions

In conclusion, our study has demonstrated for the first time that celastrol protects against testicular injury in type 2 diabetic rats by preventing the formation of proinflammatory cytokines in the testicular tissue. These findings indicate that celastrol is a potential drug for the treatment of diabetic testicular dysfunction. In addition, the TLR4/MyD88/NF-κB signaling cascade pathways could serve as a valuable novel therapeutic agent.

## DATA AVAILABILITY

All data created or analyzed during this investigation are included in the article.

## DISCLOSURES

No conflicts of interest, financial or otherwise, are declared by the authors.

## AUTHOR CONTRIBUTIONS

H.F., H.E.K., F.H.R., Y.M.E.-H., R.A., E.H.B., M.A.S., and A.E. conceived and designed research; H.F., A.A.H., R.A., E.H.B., R.I., H.A.I., A.M.E., and S.M.M. performed experiments; R.A.a., M.T.A.G., R.I., and H.A.I. analyzed data; R.A.a., M.T.A.G., R.I., and H.A.I. interpreted results of experiments; R.A.a. and M.T.A.G. prepared figures; H.F., A.A.H., H.E.K., R.A.a., F.H.R., Y.M.E.-H., R.A., R.I., H.A.I., A.M.E., S.M.M., M.A.S., and A.E. drafted manuscript; H.F., A.A.H., H.E.K., M.T.A.G., F.H.R., Y.M.E.-H., R.A., E.H.B., R.I., H.A.I., A.M.E., S.M.M., M.A.S., and A.E. edited and revised manuscript; H.F., A.A.H., H.E.K., R.A.a., M.T.A.G., F.H.R., Y.M.E.-H., R.A., E.H.B., R.I., H.A.I., A.M.E., S.M.M., M.A.S., and A.E. approved final version of manuscript.

## REFERENCES


1. **Mandal N**, **Grambergs R**, **Mondal K**, **Basu SK**, **Tahia F**, **Dagogo-Jack S.** Role of ceramides in the pathogenesis of diabetes mellitus and its complications. *J Diabetes Complications* 35: 107734, 2021. doi:10.1016/j.jdiacomp.2020.107734.
2. **Maresch CC**, **Stute DC**, **Alves MG**, **Oliveira PF**, **de Kretser DM**, **Linn T.** Diabetes-induced hyperglycemia impairs male reproductive function: a systematic review. *Hum Reprod Update* 24: 86–105, 2018. doi:10.1093/humupd/dmx033.
3. **Zhu BT.** Pathogenic mechanism of autoimmune diabetes mellitus in humans: potential role of streptozotocin-induced selective autoimmunity against human islet β-cells. *Cells* 11: 492, 2022. doi:10.3390/cells11030492.
4. **Al-Araby SQ**, **Rahman MA**, **Chowdhury MAH**, **Das RR**, **Chowdhury TA**, **Hasan CMM**, **Afroze M**, **Hashem MA**, **Hajjar D**, **Alelwani W**, **Makki AA**, **Haque MA.** Padina tenuis (marine alga) attenuates oxidative stress and streptozotocin-induced type 2 diabetic indices in Wistar albino rats. *S Afr J Bot* 128: 87–100, 2020. doi:10.1016/j.sajb.2019.09.007.
5. **Wu J**, **Yan LJ.** Streptozotocin-induced type 1 diabetes in rodents as a model for studying mitochondrial mechanisms of diabetic β cell glucotoxicity. *Diabetes Metab Syndr Obes* 8: 181–188, 2015. doi:10.2147/DMSO.S82272.
6. **Nie L**, **Cai SY**, **Shao JZ**, **Chen J.** Toll-like receptors, associated biological roles, and signaling networks in non-mammals. *Front Immunol* 9: 1523, 2018. doi:10.3389/fimmu.2018.01523.
7. **Neagu M**, **Constantin C.** Signal transduction in immune cells and protein kinases. *Adv Exp Med Biol* 1275: 133–149, 2021

[Erratum in *Adv Exp Med Biol* 1275: C1, 2021]. doi:10.1007/978-3-030-49844-3_5.

8. **Suryavanshi SV**, **Kulkarni YA.** NF-κβ: a potential target in the management of vascular complications of diabetes. *Front Pharmacol* 8: 798, 2017. doi:10.3389/fphar.2017.00798.
9. **Liu T**, **Zhang L**, **Joo D**, **Sun SC.** NF-κB signaling in inflammation. *Signal Transduct Target Ther* 2: 17023–17023, 2017. doi:10.1038/sigtrans.2017.23.
10. **Cascão R**, **Fonseca JE**, **Moita LF.** Celastrol: a spectrum of treatment opportunities in chronic diseases. *Front Med (Lausanne)* 4: 69, 2017. doi:10.3389/fmed.2017.00069.
11. **Mitrakou A**, **Kelley D**, **Mokan M**, **Veneman T**, **Pangburn T**, **Reilly J**, **Gerich J.** Role of reduced suppression of glucose production and diminished early insulin release in impaired glucose tolerance. *N Engl J Med* 326: 22–29, 1992. doi:10.1056/NEJM199201023260104.
12. **Zhu Y**, **Wan N**, **Shan X**, **Deng G**, **Xu Q**, **Ye H**, **Sun Y.** Celastrol targets adenylyl cyclase-associated protein 1 to reduce macrophages-mediated inflammation and ameliorates high fat diet-induced metabolic syndrome in mice. *Acta Pharm Sin B* 11: 1200–1212, 2021. doi:10.1016/j.apsb.2020.12.008.
13. **Nie Y**, **Fu C**, **Zhang H**, **Zhang M**, **Xie H**, **Tong X**, **Li Y**, **Hou Z**, **Fan X**, **Yan M.** Celastrol slows the progression of early diabetic nephropathy in rats via the PI3K/AKT pathway. *BMC Complement Med Ther* 20: 321, 2020. doi:10.1186/s12906-020-03050-y.
14. **Hsing AW**, **Gao YT**, **Chua S Jr**, **Deng J**, **Stanczyk FZ.** Insulin resistance and prostate cancer risk. *J Natl Cancer Inst* 95: 67–71, 2003. doi:10.1093/jnci/95.1.67.
15. **Zhang F**, **Ye C**, **Li G**, **Ding W**, **Zhou W**, **Zhu H**, **Chen G**, **Luo T**, **Guang M**, **Liu Y**, **Zhang D**, **Zheng S**, **Yang J**, **Gu Y**, **Xie X**, **Luo M.** The rat model of type 2 diabetic mellitus and its glycometabolism characters. *Exp Anim* 52: 401–407, 2003. doi:10.1538/expanim.52.401.
16. **Han LP**, **Li CJ**, **Sun B**, **Xie Y**, **Guan Y**, **Ma ZJ**, **Chen LM.** Protective effects of celastrol on diabetic liver injury via TLR4/MyD88/NF-κB signaling pathway in type 2 diabetic rats. *J Diabetes Res* 2016: 2641248, 2016. doi:10.1155/2016/2641248.
17. **Rohländer M**, **Otzen H**, **Rode K**, **Jung K**, **Schmicke M**, **Harborth T**, **Langeheine M**, **Brehm R**, **Bajcsy ÁC.** Histological comparison of testicular needle biopsy and En Bloc samples in Abattoir calves. *Animals (Basel)* 10, 2020. doi:10.3390/ani10050918.
18. **Lowry OH**, **Rosebrough NJ**, **Farr AL**, **Randall RJ.** Protein measurement with the Folin phenol reagent. *J Biol Chem* 193: 265–275, 1951.
19. **Friedewald WT**, **Levy RI**, **Fredrickson DS.** Estimation of the concentration of low-density lipoprotein cholesterol in plasma, without use of the preparative ultracentrifuge. *Clin Chem* 18: 499–502, 1972.
20. **Livak KJ**, **Schmittgen TD.** Analysis of relative gene expression data using real-time quantitative PCR and the $2^{-\Delta\Delta CT}$ method. *Methods* 25: 402–408, 2001. doi:10.1006/meth.2001.1262.
21. **Bancroft JD**, **Gamble M** (Editor)**.** *Theory and Practice of Histological Techniques*. London: Elsevier Health Science, 2008.
22. **Milosevic A**, **Bjelobaba I**, **Bozic ID**, **Lavrnja I**, **Savic D**, **Tesovic K**, **Jakovljevic M**, **Stojilkovic SS**, **Janjic MM.** Testicular steroidogenesis is suppressed during experimental autoimmune encephalomyelitis in rats. *Sci Rep* 11: 8996, 2021. doi:10.1038/s41598-021-88305-5.
23. **Mohamed EA**, **Kassem HH.** Protective effect of nebivolol on doxorubicin-induced cardiotoxicity in rats. *Arch Med Sci* 14: 1450–1458, 2018. doi:10.5114/aoms.2018.79008.
24. **Tian J**, **Zhao Y**, **Wang L**, **Li L.** Role of TLR4/MyD88/NF-κB signaling in heart and liver-related complications in a rat model of type 2 diabetes mellitus. *J Int Med Res* 49: 300060521997590, 2021. doi:10.1177/0300060521997590.
25. **La Vignera S**, **Condorelli R**, **Vicari E**, **D'Agata R**, **Calogero AE.** Diabetes mellitus and sperm parameters. *J Androl* 33: 145–153, 2012. doi:10.2164/jandrol.111.013193.
26. **Al-Megrin WA**, **El-Khadragy MF**, **Hussein MH**, **Mahgoub S**, **Abdel-Mohsen DM**, **Taha H**, **Bakkar AAA**, **Abdel Moneim AE**, **Amin HK.** Green *Coffea arabica* extract ameliorates testicular injury in high-fat diet/streptozotocin-induced diabetes in rats. *J Diabetes Res* 2020: 6762709, 2020. doi:10.1155/2020/6762709.
27. **Pournaghi P**, **Sadrkhanlou RA**, **Hasanzadeh S**, **Foroughi A.** An investigation on body weights, blood glucose levels and pituitary-gonadal axis hormones in diabetic and metformin-treated diabetic female rats. *Vet Res Forum* 3: 79–84, 2012.
28. **Zhang M**, **Chen Y**, **Yang MJ**, **Fan XR**, **Xie H**, **Zhang L**, **Nie YS**, **Yan M.** Celastrol attenuates renal injury in diabetic rats via MAPK/NF-κB pathway. *Phytother Res* 33: 1191–1198, 2019. doi:10.1002/ptr.6314.
29. **Abu Bakar MH**, **Mohamad Khalid MSF**, **Nor Shahril NS**, **Shariff KA**, **Karunakaran T.** Celastrol attenuates high-fructose diet-induced inflammation and insulin resistance via inhibition of 11β-hydroxysteroid dehydrogenase type 1 activity in rat adipose tissues. *BioFactors* 48: 111–134, 2022. doi:10.1002/biof.1793.
30. **Chung SS**, **Ho EC**, **Lam KS**, **Chung SK.** Contribution of polyol pathway to diabetes-induced oxidative stress. *J Am Soc Nephrol* 14: S233–S236, 2003. doi:10.1097/01.asn.0000077408.15865.06.
31. **Balaban RS**, **Nemoto S**, **Finkel T.** Mitochondria, oxidants, and aging. *Cell* 120: 483–495, 2005. doi:10.1016/j.cell.2005.02.001.
32. **Naas H**, **de Oliveira AA**, **Karpova T**, **Nunes KP.** Toll-like receptor 4 (TLR4) as a possible pathological mechanism in hyperglycemia-associated testicular dysfunction. *Med Hypotheses* 127: 116–119, 2019. doi:10.1016/j.mehy.2019.04.010.
33. **Bhushan S**, **Tchatalbachev S**, **Klug J**, **Fijak M**, **Pineau C**, **Chakraborty T**, **Meinhardt A.** Uropathogenic *Escherichia coli* block MyD88-dependent and activate MyD88-independent signaling pathways in rat testicular cells. *J Immunol* 180: 5537–5547, 2008. doi:10.4049/jimmunol.180.8.5537.
34. **Feng H**, **Su R**, **Song Y**, **Wang C**, **Lin L**, **Ma J**, **Yang H.** Positive correlation between enhanced expression of TLR4/MyD88/NF-κB with insulin resistance in placentae of gestational diabetes mellitus. *PLoS One* 11: e0157185, 2016. doi:10.1371/journal.pone.0157185.
35. **Mehal WZ.** The inflammasome in liver injury and non-alcoholic fatty liver disease. *Dig Dis* 32: 507–515, 2014. doi:10.1159/000360495.
36. **Liu X**, **Lu J**, **Liao Y**, **Liu S**, **Chen Y**, **He R**, **Men L**, **Lu C**, **Chen Z**, **Li S**, **Xiong G**, **Yang S.** Dihydroartemisinin attenuates lipopolysaccharide-induced acute kidney injury by inhibiting inflammation and oxidative stress. *Biomed Pharmacother* 117: 109070, 2019. doi:10.1016/j.biopha.2019.109070.
37. **Al-Harbi NO**, **Nadeem A**, **Ahmad SF**, **Alanazi MM**, **Aldossari AA**, **Alasmari F.** Amelioration of sepsis-induced acute kidney injury through inhibition of inflammatory cytokines and oxidative stress in dendritic cells and neutrophils respectively in mice: role of spleen tyrosine kinase signaling. *Biochimie* 158: 102–110, 2019. doi:10.1016/j.biochi.2018.12.014.
38. **Gill R**, **Tsung A**, **Billiar T.** Linking oxidative stress to inflammation: toll-like receptors. *Free Radic Biol Med* 48: 1121–1132, 2010. doi:10.1016/j.freeradbiomed.2010.01.006.
39. **Chen X**, **Wei W**, **Li Y**, **Huang J**, **Ci X.** Hesperetin relieves cisplatin-induced acute kidney injury by mitigating oxidative stress, inflammation and apoptosis. *Chem Biol Interact* 308: 269–278, 2019. doi:10.1016/j.cbi.2019.05.040.
40. **Li C**, **Che LH**, **Ji TF**, **Shi L**, **Yu JL.** Effects of the TLR4 signaling pathway on apoptosis of neuronal cells in diabetes mellitus complicated with cerebral infarction in a rat model. *Sci Rep* 7: 43834, 2017. doi:10.1038/srep43834.
41. **Cascão R**, **Vidal B**, **Raquel H**, **Neves-Costa A**, **Figueiredo N**, **Gupta V**, **Fonseca JE**, **Moita LF.** Effective treatment of rat adjuvant-induced arthritis by celastrol. *Autoimmun Rev* 11: 856–862, 2012. doi:10.1016/j.autrev.2012.02.022.
42. **Allison AC**, **Cacabelos R**, **Lombardi VR**, **Alvarez XA**, **Vigo C.** Celastrol, a potent antioxidant and anti-inflammatory drug, as a possible treatment for Alzheimer's disease. *Prog Neuropsychopharmacol Biol Psychiatry* 25: 1341–1357, 2001. doi:10.1016/s0278-5846(01)00192-0.
43. **Wang Y**, **Li C**, **Gu J**, **Chen C**, **Duanmu J**, **Miao J**, **Yao W**, **Tao J**, **Tu M**, **Xiong B**, **Zhao L**, **Liu Z.** Celastrol exerts anti-inflammatory effect in liver fibrosis via activation of AMPK-SIRT3 signalling. *J Cell Mol Med* 24: 941–953, 2020. doi:10.1111/jcmm.14805.
44. **Zhang B**, **Zhong Q**, **Chen X**, **Wu X**, **Sha R**, **Song G**, **Zhang C**, **Chen X.** Neuroprotective effects of celastrol on transient global cerebral ischemia rats via regulating HMGB1/NF-κB signaling pathway. *Front Neurosci* 14: 847, 2020 [Erratum in *Front Neurosci* 15: 637004, 2021]. doi:10.3389/fnins.2020.00847.
45. **Bauché F**, **Fouchard MH**, **Jégou B.** Antioxidant system in rat testicular cells. *FEBS Lett* 349: 392–396, 1994. doi:10.1016/0014-5793(94)00709-8.
46. **Jannuzzi AT**, **Kara M**, **Alpertunga B.** Celastrol ameliorates acetaminophen-induced oxidative stress and cytotoxicity in HepG2 cells. *Hum Exp Toxicol* 37: 742–751, 2018. doi:10.1177/0960327117734622.

47. **Li YH**, **Liu SB**, **Zhang HY**, **Zhou FH**, **Liu YX**, **Lu Q**, **Yang L.** [Antioxidant effects of celastrol against hydrogen peroxide-induced oxidative stress in the cell model of amyotrophic lateral sclerosis]. *Sheng li xue Bao* 69: 751–758, 2017.
48. **Tesone M**, **Oliveira-Filho RM**, **Valle LB**, **Calvo JC**, **Barañao JL**, **Foglia VG**, **Charreau EH.** Androgen receptors in the diabetic rat. *Diabetologia* 18: 385–390, 1980. doi:10.1007/BF00276819.
49. **Fushimi H**, **Inoue T**, **Ohtsuka A**, **Kanao K**, **Ishihara S**, **Tsujimura T**, **Nunotani H**, **Minami T**, **Okazaki Y.** Plasma and testicular testosterone in experimental diabetic rats. *Diabetes Res Clin Pract* 3: 81–84, 1987. doi:10.1016/s0168-8227(87)80011-6.
50. **Al-Khamas JH.** Effect of cinnamon zeylanicum bark water extract on male diabetic albino rats fertility. *Bas J Vet Res* 17: 123–135, 2018.
51. **Faddladdeen KAJ.** The possible protective and therapeutic effects of ginger and cinnamon on the testis and coda epididymis of streptozotocin-induced-diabetic rats: histological and biochemical studies. *Saudi J Biol Sci* 29: 103452, 2022. doi:10.1016/j.sjbs.2022.103452.
52. **Harakeh S**, **Qari M**, **Rajeh N**, **Ali S**, **El-Shitany N**, **Hassan S**, **Abd-Allah EA**, **Tashkandi H**, **Malik MFA**, **Aljabri FK**, **Azhar L**, **Azhar N**, **Al-Jaouni S**, **Almehmadi Y**, **Alamri T**, **Mousa S.** Ellagic acid nanoparticles attenuate oxidative stress and testicular damage in high fat diet/streptozotocin-induced diabetic rats. *J King Saud Univ Sci* 34: 101720, 2022. doi:10.1016/j.jksus.2021.101720.
53. **Zhang C**, **Zhao M**, **Wang B**, **Su Z**, **Guo B**, **Qin L**, **Zhang W**, **Zheng R.** The Nrf2-NLRP3-caspase-1 axis mediates the neuroprotective effects of celastrol in Parkinson's disease. *Redox Biol* 47: 102134, 2021. doi:10.1016/j.redox.2021.102134.
54. **Song J**, **He GN**, **Dai L.** A comprehensive review on celastrol, triptolide and triptonide: Insights on their pharmacological activity, toxicity, combination therapy, new dosage form and novel drug delivery routes. *Biomed Pharmacother* 162: 114705, 2023. doi:10.1016/j.biopha.2023.114705.
55. **Jing M**, **Yang J**, **Zhang L**, **Liu J**, **Xu S**, **Wang M**, **Zhang L**, **Sun Y**, **Yan W**, **Hou G**, **Wang C**, **Xin W.** Celastrol inhibits rheumatoid arthritis through the ROS-NF-κB-NLRP3 inflammasome axis. *Int Immunopharmacol* 98: 107879, 2021. doi:10.1016/j.intimp.2021.107879.